Adsorption (2013) 19:959–966
DOI 10.1007/s10450-013-9504-9

Adsorption of SO_2 by typical carbonaceous material: a comparative study of carbon nanotubes and activated carbons

**Fei Sun · Jihui Gao · Yuwen Zhu · Guoqing Chen ·
Shaohua Wu · Yukun Qin**

Received: 27 December 2011 / Accepted: 4 February 2013 / Published online: 20 February 2013

Abstract Applying activated carbons for SO_2 adsorption and conversion to H_2SO_4, as a dry process, has been considered the development direction of desulfurization technology. Coal-based activated carbon, coconut shell activated carbon, single wall carbon nanotube and multi-wall carbon nanotubes were used as typical carbonaceous materials to study the SO_2 adsorption mechanism. SEM, N_2 adsorption, XPS and fixed-bed reaction system were employed to study the morphology, pore structure, surface functional groups and SO_2 adsorption behaviors of the four adsorbents. The fixed-bed experiment was carried out at normal pressure and SO_2 concentration was set 1,000 ppm. According to SEM and N_2 adsorption results, hierarchical pore structure was an important characteristic of activated carbon. Aggregation was an important characteristic of CNTs. Mesopores and macropores took the dominance of pore structure in CNTs. According the SO_2 adsorption data and correlation analysis, it can be concluded that the dominant adsorption type on activated carbons does not alter with adsorption temperature changing. However, the adsorption type of SO_2 adsorption on CNTs changes with adsorption temperature varying. With adsorption temperature increasing, the dominant adsorption type transforms to chemisorption by physisorption. Higher-density π–π* in carbon nanotubes may be the active sites for the SO_2 chemical adsorption. Micropores with the diameter smaller than 0.7 nm were the best SO_2 adsorption place for both activated carbons and carbon nanotubes. The results provided a profound insight into the microstructure and SO_2 adsorption mechanism of the two kinds of carbonaceous materials.

Keywords SO_2 adsorption · Activated carbon · Carbon nanotube · π–π* · Physical adsorption · Chemical adsorption

Abbreviation

CBAC	Coal-based activated carbon
CSAC	Coconut shell activated carbon
CNTs	Carbon nanotubes
SWNT	Single wall carbon nanotube
MWNT	Multi-wall carbon nanotube

1 Introduction

Coal is the major resource in China (Xu 2007). Sulfur dioxide (SO_2) emission from coal combustion in power plant is one of the major anthropogenic contributors to air pollution (Sakizci et al. 2011). Traditional wet desulfurization of flue gas using limestone has been commercialized for a long time. However, it has some disadvantages of high capital cost, requiring large amount of water, SO_2 not completely removing with 50 ppm leaking out etc. (Mochida et al. 2000). More importantly, the by-product gypsum of wet desulfurization shows a low commercial value due to China's rich gypsum resources and was mostly abandoned. In recent years, applying activated

---

National Natural Science Foundation–Shenhua Group, "Coal Joint Fund" (Grant No. 51134015); National Natural Science Foundation of China (Grant No. 50806019).

F. Sun (✉) · J. Gao (✉) · Y. Zhu · G. Chen · S. Wu · Y. Qin
School of Energy Science and Engineering, Harbin Institute of Technology, 92 West Straight Street, Harbin 150001, People's Republic of China
e-mail: sunfll@126.com

J. Gao
e-mail: gaojh@hit.edu.cn

carbons for SO_2 adsorption and conversion to H_2SO_4, as a dry process, has attracted many researchers' attention (Mochida et al. 2000; Davini 1990; Lizzio et al. 1997; Rubio et al. 1998; Zhang et al. 2002; Liu et al. 2003; Gaur et al. 2006; Raymundo-Piñero et al. 2001). Previous researchers have done a lot of work on SO_2 removal by activated carbons. However, due to the complexity of surface micro-structure of activated carbons, the multi reaction components and the complex intermediate steps during the SO_2 transformation process, there is still no uniform conclusion on the SO_2 removal mechanism in the activated carbon interior (Mochida et al. 2000; Davini 1990; Lizzio et al. 1997; Rubio et al. 1998; Zhang et al. 2002; Liu et al. 2003; Gaur et al. 2006; Raymundo-Piñero et al. 2001; Zawadzki 1987).

SO_2 adsorption is the first step of subsequent oxidation and sulfuric acid forming reaction. Most scholars believe that SO_2 dry adsorption process includes both physical adsorption and chemical adsorption two steps. Lizzio and his coworkers' studies (1997) have shown that the SO_2 adsorption capacities of activated carbons have no necessary relationship with specific areas of activated carbons indicating that the physical adsorption does not play the major role. However, Rubio, Izquierdo et al. (1997, 1998) and Zhang et al. (2004), etc. held that the SO_2 adsorption properties depend on the specific area of activated carbons. Davini (1990, 1999) suggested that the amount of surface basic sites determine the SO_2 adsorption property and pore structure has less influence on the SO_2 adsorption. From above analyses, it can be seen that the effect mechanism of pore structure and surface chemistry of activated carbons on the SO_2 adsorption process is still ill-defined. Further research on SO_2 dry adsorption is needed to get a clear understanding of the adsorption type and influencing factors of SO_2 dry adsorption.

Carbon nanotubes (CNTs), as newly emerged carbonaceous materials have attracted massive attention for their potential utilization in the gas adsorption or water treatment (Iijima 1991; Gayathri et al. 2007; Mahdizadeh et al. 2011; Long and Yang 2001; Peng and Li 2003; Lu and Chung 2005). Compared with activated carbon materials, the internal pore structure of CNTs is simple and uniform. Moreover, the chemical natures of CNTs are consistent due to the high degree of graphitization. Therefore, taking carbon nanotubes as contrast materials and analyzing SO_2 adsorption behavior on CNTs will be of great values to understand the SO_2 adsorption mechanism by activated carbons.

The objective of this study was to elucidate the difference of the SO_2 adsorption behaviors between activated carbons and CNTs by coupling adsorption temperature, pore structure and surface chemistry with SO_2 adsorption data. The pore structure parameters and surface functional groups of different adsorbents were examined to understand the factors controlling the SO_2 adsorption of CNTs and activated carbons and to provide an insight into the SO_2 adsorption of the two kinds of carbonaceous materials. Moreover, the correlations between micropore structure parameters of adsorbents and their SO_2 adsorption capacities were examined to determine which kind of micropores is suitable for SO_2 molecules entering and adsorption.

2 Experimental section

2.1 Materials

Coconut shell activated carbon (CSAC for short, from Lieyang Chaoyang activated carbon Co., Ltd), coal-based activated carbon (CBAC, from Inner Mongolia Sinovac Alashan coal industry Co., Ltd), single wall carbon nanotube (SWNT, outer diameter: <2 nm, length: 5–15 μm, purity >90 %, from Shenzhen Nanotech Port Co., Ltd), multi-wall carbon nanotube (MWNT, outer diameter: <10 nm, length: 5–15 μm, purity >95 %, from Shenzhen Nanotech Port Co., Ltd) were used as received. Prior to use, CSAC and CBAC were grounded to particles with the size in the range of 250–500 μm. The selected samples represent typical types of activated carbon materials and carbon nanotubes.

2.2 Methods

2.2.1 SO_2 saturation adsorption test

The SO_2 adsorption test has been carried out at 303–393 K using a fixed-bed experimental system which is illustrated in Fig. 1. It consists of a fixed-bed glass reactor (1.2 cm diameter), placed in a vertical furnace, with a system of valves and mass flow controllers which allow to control the flow rate and the composition of the reactor inlet gas. Portable FTIR (DX4000) produced by Finland Gasmet Company was used to online monitor the SO_2 concentration of reactor inlet and outlet. In a typical run, 1 g of samples was packed into the glass column. Subsequently required gas (1,000 ppm SO_2, N_2 balance, total flow rate 1 L/min) was introduced into the reactor after the temperature in the reaction zone reached the desired value and kept a steady state. The test lasted until the SO_2 concentration kept constant and reached adsorption saturation. The SO_2 removal efficiency was defined as:

$$\mathrm{DeSO_2}(\%) = \frac{\mathrm{SO_2(in)} - \mathrm{SO_2(out)}}{\mathrm{SO_2(in)}} \times 100\,\% \qquad (1)$$

where SO_2 (in) and SO_2 (out) were inlet SO_2 concentration and outlet SO_2 concentration respectively measured by FTIR. Saturation sulfur retention of samples was calculated

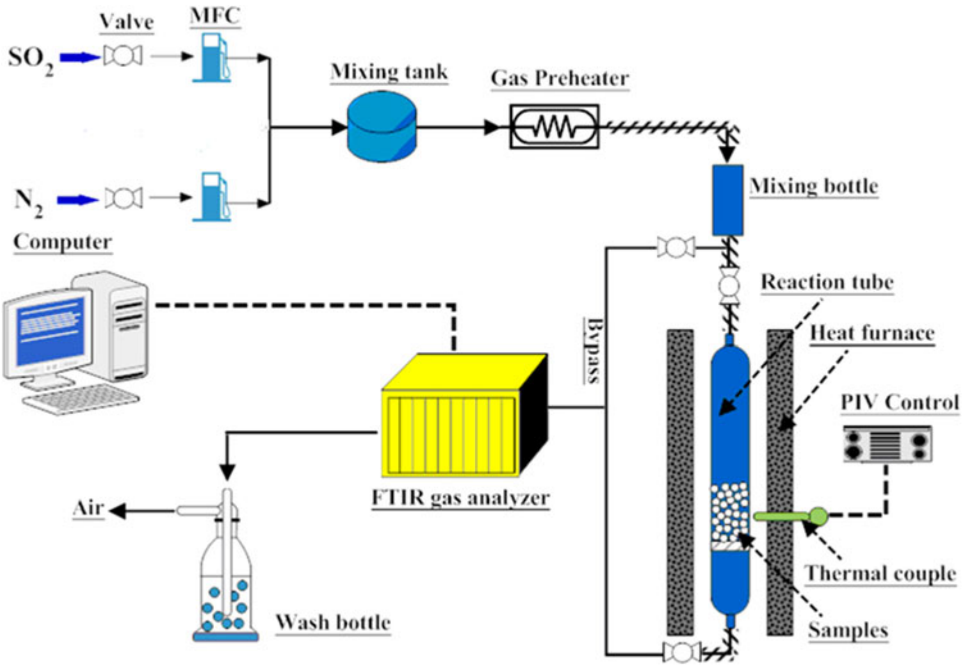

Fig. 1 Scheme of SO_2 adsorption equipment: the fixed-bed reactor was the main body of experiment system. The names of relevant experimental equipment were marked in the figure

by integrating the area above the saturation curves and saturation time. For each sample, the SO_2 test was repeated at least twice and the determined capacities agreed to within 4 %.

2.2.2 *Morphology and pore structure characterization*

The surface morphology of carbonaceous materials was analyzed by using scanning electron microscopy (JSM-7401F). The pore structure characteristic of carbonaceous materials was determined by nitrogen adsorption at 77.35 K using automatic Micromeritics ASAP 2020 volumetric sorption analyzer. The BET surface area was calculated from the isotherm using the Brunauer–Emmett–Teller equation. The micropore surface and micropore volume were calculated by t-plot method. The micropore volume with the diameter smaller than 0.7 nm was determined using the HK pore size distribution method and the micropore volumes with the diameter 0.7–1.0 and 1.0–2.0 nm were determined using the DFT pore size distribution method. Each sample in our research was tested for three times and the results of three times are almost identical.

2.2.3 *Surface chemistry characterization*

XPS characterization of surface chemistry of four carbonaceous materials was carried out on a Thermofisher Scientific K-Alpha spectrometer using AlKa X-ray at 12 kV and 6 mA. The pressure inside the vacuum system was maintained at 10^{-8} mbar. The values of binding energy (BE) were calibrated with respect to C 1*s* peak at 284.6 eV. A software package Advantage 4.75 was used for C 1*s* spectra peak fitting and quantification. In this study, different forms of carbon-containing functional group were analyzed.

3 Results and discussion

3.1 Pore structure and surface chemistry characterization

3.1.1 *Morphology of carbonaceous materials*

Figure 2 shows the SEM micrographs of activated carbons (CBAC and CSAC). It can be seen that the surface of CBAC, which was prepared from coal, is severely uneven and irregular. It can be attributed to the erosion of carbon during carbonization and activation process. Compared with CBAC, the surface of CSAC prepared from coconut is smooth. It can be seen that massive circular pores arrange on the surface of CSAC regularly. The size of these pores was calculated as marked in Fig. 2a, b. The pores in CBAC (size of 54 nm) and CSAC (size of 60 nm) both belong to macropores (>50 nm). SEM micrographs of CNTs are shown in Fig. 3a, b. It can be seen clearly that both SWNTs and MWNTs aggregate to be bundles. Aggregation is an important characteristic that differentiates CNTs from other carbonaceous adsorbents (e.g., activated carbons, carbon fibers) (Zhang and Shao 2009). CNTs are prone to aggregation due to the strong van der Waals interactions

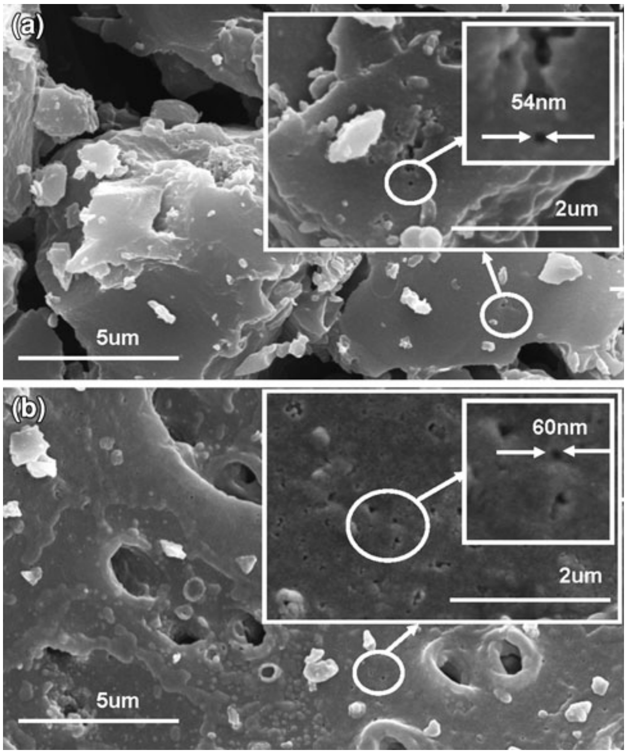

Fig. 2 Morphology of activated carbons by SEM: **a** SEM micrographs of coal-based activated carbon (CBAC); **b** SEM micrographs of coconut shell activated carbon (CSAC)

between carbon macromolecules. On one hand, aggregation can lead to the reduction in surface area which has a potential negative impact on the SO_2 adsorption. On the other hand, aggregation leads to the generation of interstitial channels between nanotubes and grooves on the periphery of CNT bundles which have positive impacts on the SO_2 adsorption. The detailed differences among their structural characteristic were further elucidated by obtaining nitrogen adsorption isotherms at 77.35 K.

3.1.2 Pore structure characterization

The nitrogen adsorption isotherms of four adsorbents are shown in Fig. 4. Adsorption isotherm of CSAC shows the typical type-I feature indicating the presence of large fractions of micropores. The isotherm pattern of CBAC behaves both type-I and type-II features which shows both microporous and macroporous characteristics (Xin et al. 2010). Compared to activated carbons, the isotherms of CNTs contain obvious hysteresis loops, demonstrating that capillary condensation is one of the adsorption mechanisms for nitrogen adsorption. It indicates that CNTs show mesoporous characteristics. The isotherm pattern of MWNT suggests it has less micropores and mesopores than SWNT.

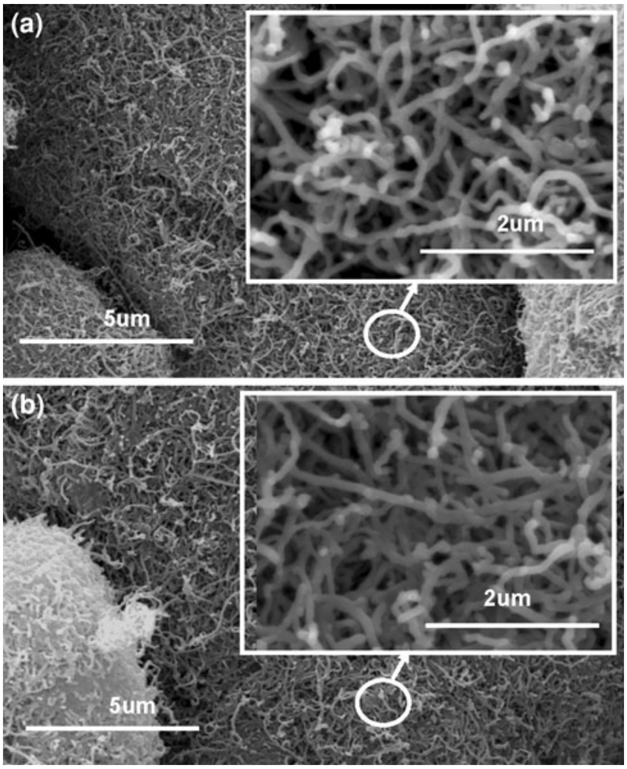

Fig. 3 Morphology of carbon nanotubes by SEM: **a** SEM micrographs of single wall carbon nanotube (SWNT); **b** SEM micrographs of multi-wall carbon nanotube (MWNT)

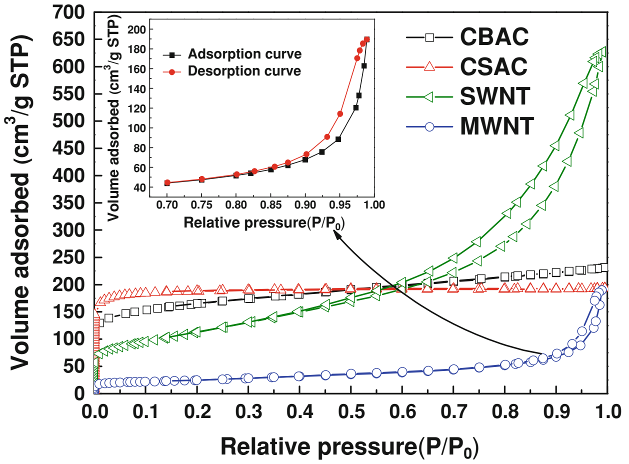

Fig. 4 Nitrogen adsorption isotherms of coal-based activated carbon (CBAC), coconut shell activated carbon (CSAC), single wall carbon nanotube (SWNT) and multi-wall carbon nanotube (MWNT)

The detailed pore structure parameters: BET surface areas (S_{BET}), micropore surface areas (S_{mic}), total pore volume (V_t), micropore volume (V_{mic}), microporosity (V_{mic}/V_t) and micropore size distributions of adsorbents are summarized in Table 1. It can be seen that more than 67 % of nitrogen adsorption in the CBAC and 96 % in the CSAC are due to the micropore adsorption, whereas only 17 % in

Table 1 Pore structure parameters from nitrogen adsorption of four adsorbents

Sample	S_{BET} (m^2/g)	S_{mic} (m^2/g)	V_t (cm^3/g)	V_{mic} (cm^3/g)	V_{mic}/V_t	Micropore volume distribution		
						$V_{<0.7\ nm}$ (cm^3/g)	$V_{0.7–1\ nm}$ (cm^3/g)	$V_{1–2\ nm}$ (cm^3/g)
CBAC	563	308	0.354	0.237	0.672	0.141	0.037	0.059
CSAC	748	671	0.298	0.286	0.960	0.183	0.042	0.061
SWNT	404	41	0.859	0.148	0.172	0.033	0.056	0.059
MWNT	87	21	0.186	0.034	0.183	0.006	0.015	0.013

the SWNT and 18 % in the MWNT. It is well known that mesopores and macropores have higher pore volume to surface areas ratios than those of micropores. Therefore, the larger proportion of mesopores and macropores in CNTs results in larger pore volumes but relatively smaller surface areas than those of CBAC and CSAC whose micropores take the dominant status among pore structure. As shown in Table 1, SWNT has the largest total pore volume while its BET surface area is much smaller than CBAC and CSAC.

3.1.3 *Surface chemistry analysis*

Surface functional groups are by far the most important factors influencing the surface chemical characteristics of carbonaceous materials and they are the active sites for SO_2 chemisorption in carbonaceous materials. In the current investigations, the peak fitting of C 1*s* spectra by XPS were made to obtain the difference of surface functional species and content between ACs and CNTs. The results are given in Table 2. According to preliminary research results (Rodriguez-Reinoso 1998; Li et al. 2001), the C 1*s* spectra of carbonaceous materials in this investigation can be resolved into five component peaks representing graphitic carbon (C–C, BE = 284.2 eV); carbon in alcohol, ether or phenol groups (C–O, BE = 285.5 eV); carbonyl or quinone groups (C=O, BE = 286.7–287.8 eV); carboxyl or ester groups (O=C–O, BE = 288.3–289.3 eV); delocalized π-bonds in aromatic rings (π–π*, BE = 291.2 eV). As listed in Table 2, it can be seen that the relative intensity of graphitic carbon of SWNT and MWNT are much higher than CBAC and CSAC and the amount of oxygen binding with carbon atom of CNTs show a significant lower level than activated carbons (seen from atomic ration of [O]/[C]). In addition, it can be seen that the amount of π–π* in SWNT (7.24 %) and MWNT (6.73 %) are obviously higher than CBAC (5.33 %) and CSAC (3.56 %).

3.2 SO_2 adsorption on carbonaceous materials

The SO_2 saturation adsorption curve of CBAC at different reaction temperatures are presented in Fig. 5. The calculated sulfur capacities of four adsorbents under different conditions are collected in Table 3.

As illustrated in Fig. 5, the temperature has a great impact on the SO_2 adsorption on CBAC. CSAC shows the similar SO_2 adsorption characteristic. As shown in Fig. 5 and Table 3, it can be seen that the saturation adsorption time for CBAC and CSAC gradually decreases as the temperature increases. As the temperature increases, the adsorption curve of CBAC moves inward and the adsorption capacity declines rapidly. According to above analysis, it is obvious that physical adsorption is the main adsorption type during SO_2 adsorption process on CBAC and CSAC.

Moreover, we use dimensionless sulfur capacity (defined as the ratios of SO_2 capacities of four adsorbents at 333, 363, 393 K to those at 303 K) to characterize the changes of SO_2 adsorption capacities with the increase of temperature. The dimensionless sulfur capacities of the four adsorbents varied with temperature are illustrated in Fig. 6. It can be seen that dimensionless sulfur capacity of CSAC declines more slowly than that of CBAC. The reason can be attributed to the difference of pore structure between CBAC and CSAC. SO_2 adsorption mainly takes place in micropore in which a strong potential energy fields can be formed. The strong potential energy fields can lead to easy adsorption and on the contrary lead to difficult desorption. In Sect. 3.1.2, it can be found that CSAC has much richer micropores than CBAC. Therefore, a higher desorption resistance in CSAC leads to a relatively weaker temperature sensitivity of SO_2 adsorption comparing to CBAC.

Compared to CBAC and CSAC, the SO_2 adsorption behaviors of SWNT and MWNT at different adsorption temperatures show great differences as presented in Table 3 and Fig. 6. For both SWNT and MWNT, the SO_2 adsorption behaviors varied with temperature can be described as follows: (i) when the temperature increases from 303 to 333 K, the saturation adsorption time and the SO_2 saturation capacity decrease obviously that is similar to CBAC and CSAC; (ii) when the temperature increases from 333 to 393 K, the saturation adsorption time and the SO_2 saturation capacity gradually increases that is opposite to CBAC and CSAC.

Based on the adsorption phenomenon found in CNTs, we believe that the SO_2 adsorption on CNTs is not

Table 2 XPS curve-fit data for C 1*s* peaks of activated carbons and carbon nanotubes

Samples	Binding states of carbon and oxygen (%)					Atomic ratio [O]/[C]
	–C–C–	–C–O–	C=O	O=C–O	π–π*	
CBAC	69.63	9.26	6.50	6.68	5.33	0.074
CSAC	57.50	15.49	14.65	9.19	3.56	0.078
SWNT	73.79	8.69	5.89	3.40	7.24	0.021
MWNT	76.70	7.06	2.01	5.86	6.73	0.017

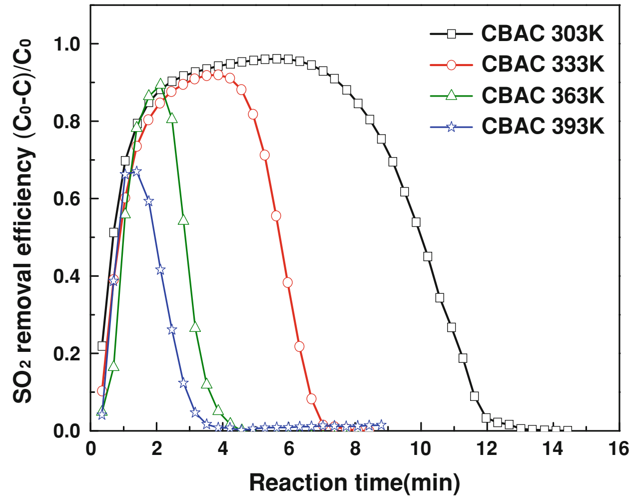

Fig. 5 SO_2 saturation adsorption curve for CBAC at different reaction temperatures (303–393 K) Reaction conditions: 1 g of adsorbents, 1000 ppm SO_2, N_2 balance, flow rate 1 L/min

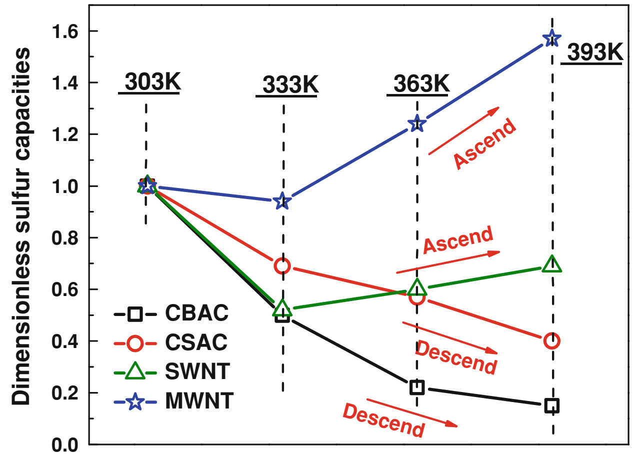

Fig. 6 Dimensionless sulfur capacities for the four adsorbents variation with temperature (It can be seen that CNTs shows a great difference comparing to activated carbons as the temperature increases from 333–393 K)

Table 3 Saturation adsorption time and SO_2 saturation capacities calculated by integrating the area above the saturation curves and the saturation time for four adsorbents

Samples	Reaction temperature (K)	Saturation adsorption time (min)	SO_2 saturation capacity (mg/g)
CBAC	303	12	12.21
	333	7	6.07
	363	4.5	2.63
	393	3.5	1.79
CSAC	303	17.5	21.21
	333	15	14.56
	363	12.5	12.03
	393	8	8.59
SWNT	303	6	3.51
	333	4	1.83
	363	5	2.09
	393	5.5	2.42
MWNT	303	4	1.04
	333	4	0.98
	363	5.2	1.29
	393	7.5	1.63

dominant by only one adsorption type: (i) in the low temperature range (from 303 to 333 K), the SO_2 adsorption is dominated by physical adsorption and the adsorption properties decrease with the increase of adsorption temperature; (ii) in the relative high temperature range, the chemical adsorption begins to play a leading role and therefore, the SO_2 adsorption properties of CNTs increase when adsorption temperature increases from 333 to 393 K. From Table 2 we can see that the amount of π–π* in SWNT (7.24 %) and MWNT (6.73 %) are obviously higher than CBAC (5.33 %) and CSAC (3.56 %). It has been founded in previous studies that π electron systems may take part in making up the Lewis basic sites which can chemically adsorb acid gases (Zawadzki 1987; Zhang et al. 2004). Therefore, we think the higher-density π–π* in CNTs may be the active sites for SO_2 chemical adsorption in the higher temperature range.

Meanwhile, it can be discovered from Fig. 6 that the ascendant amplitude of the SO_2 chemical adsorption capacities as the temperature increases from 333 to 393 K is lower than the descent amplitude of the SO_2 physical adsorption capacities as the temperature increases from 303 to 333 K. This indicates that the temperature sensitivity of

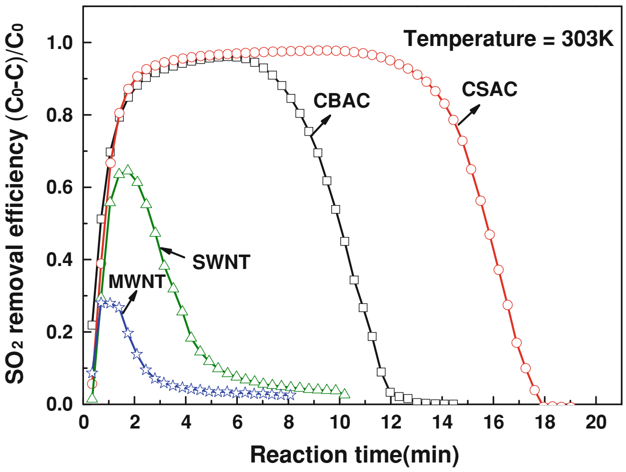

Fig. 7 SO_2 saturation adsorption curves for four adsorbents at 303 K. Reaction conditions: 1 g of adsorbents, 1000 ppm SO_2, N_2 balance, flow rate 1 L/min

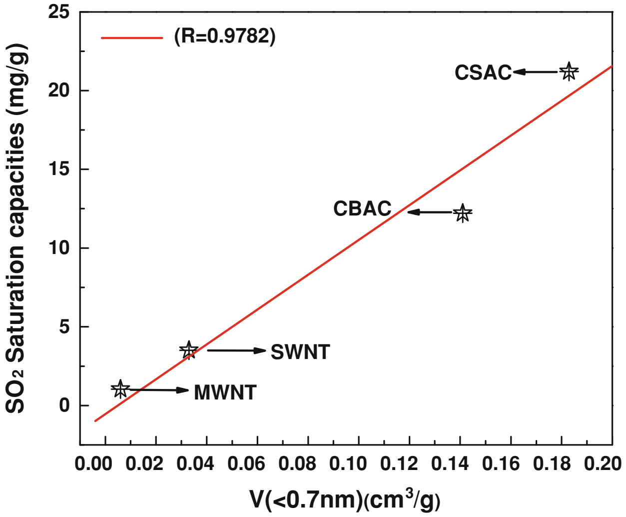

Fig. 8 Dependence of saturation sulfur capacities for four carbonaceous materials at 303 K on the volumes of micropores with the diameter smaller than 0.7 nm (The saturation sulfur capacities show a remarkably good correlation with the micropores smaller than 0.7 nm with correlation coefficient R = 0.98)

SO_2 chemical adsorption is weaker than that of the SO_2 physical adsorption for CNTs.

In order to understand the differences of the SO_2 physical adsorption performance between four carbonaceous materials, the SO_2 saturation adsorption curves for the four adsorbents at 303 K are investigated in Fig. 7. It can be seen that ACs show evidently better adsorption property than CNTs. Adsorption platforms with 100 % adsorption efficiency can be found in adsorption curves of CBAC and CSAC while SWNT and MWNT do not show the characteristic. Since SO_2 molecule diameter is 0.411 nm, not all micropores (<2 nm) are suitable for SO_2 adsorption. In order to further understand which aperture micropore is suitable for SO_2 molecules entering and adsorption, we divided the micropore of the four adsorbents into three kinds of pores based on pore diameter: smaller than 0.7 nm, 0.7–1.0 nm and 1.0–2.0 nm. Different ranges of micropore volumes were summarized in Table 1. The dependence of the saturation sulfur capacities of the four carbonaceous materials at 303 K on micropore volumes of three pore sizes were presented in Fig. 8 to explain which kind of micropore governs the SO_2 physical adsorption.

As illustrated in Fig. 8, the saturation sulfur capacities of the four carbonaceous materials show a remarkably good correlation with the micropores with the diameter smaller than 0.7 nm with correlation coefficient R = 0.98. At the meanwhile, the saturation sulfur capacities have no inevitable relationship with micropores 0.7–1 and 1–2 nm. Wider pore size distribution is not conducive to the creation of adsorption potential energy field and accordingly is not conducive to SO_2 adsorption. On top of above analysis, it can be concluded that the micropores whose diameter are smaller than 0.7 nm are the best pore structure for the SO_2 adsorption by carbonaceous materials.

4 Conclusions

In this study, the microstructure, the surface chemistry and the SO_2 adsorption behaviors of activated carbons and CNTs were investigated. It was found that hierarchical pore structure was an important characteristic of activated carbon. Aggregation was an important characteristic of CNTs. Mesopores and macropores took the dominance of pore structure in CNTs. The dominant adsorption type on activated carbons does not alter with adsorption temperature changing. However, the adsorption type of SO_2 adsorption on CNTs changes with adsorption temperature varying. With adsorption temperature increasing, the dominant adsorption type transforms to chemisorption by physisorption. The higher-density π–π^* in CNTs might be the active sites for SO_2 chemical adsorption, the micropores smaller than 0.7 nm were the best SO_2 adsorption place for both activated carbons and CNTs. Based on the SO_2 adsorption mechanism of the four adsorbents, our next research is to investigate SO_2 oxidation and SO_3 hydration mechanism in the presence of O_2 and H_2O by using activated carbons and CNTs as adsorbents.

Acknowledgments This research was financially supported by the National Natural Science Foundation of China (Grant No. 50806019) and National Natural Science Foundation–Shenhua Group, "Coal Joint Fund" (Grant No. 51134015).

References

Davini, P.: Adsorption and desorption of SO_2 on active carbon: The effect of surface basic groups. Carbon **28**, 565–571 (1990)

Davini, P.: Desulfurization properties of active carbons obtained from petroleum pitch pyrolysis. Carbon **37**, 1363–1371 (1999)

Gaur, V., Asthan, R., Verma, N.: Removal of SO_2 by activated carbon fibers in the presence of O_2 and H_2O. Carbon **44**, 46–60 (2006)

Gayathri, V., Geetha, R.: Hydrogen adsorption in defected carbon nanotubes. Adsorption **13**, 53–59 (2007)

Iijima, S.: Helical microtubules of graphitic carbon. Nature **354**, 56–58 (1991)

Li, K.X., Ling, L.C., Lu, C.X., Qiao, W.M., Liu, Z.Y.: Catalytic removal of SO_2 over ammonia-activated carbon fibers. Carbon **39**, 1803–1808 (2001)

Liu, Q.Y., Guan, J.S., Li, J.G., Li, C.H.: SO_2 removal from flue gas by activated semi-cokes 2: Effects of physical structure and chemical properties on SO_2 removal activity. Carbon **41**, 2225–2230 (2003)

Lizzio, A.A., DeBarr, J.A.: Mechanism of SO_2 removal by carbon. Energy Fuels **11**, 284–291 (1997)

Long, R.Q., Yang, R.T.: Communications to the Editor: Carbon nanotubes as superior sorbent for dioxin removal. J. Am. Chem. Soc. **123**, 2058–2059 (2001)

Lu, C.S., Chung, Y.L., Chang, K.F.: Adsorption of trihalomethanes from water with carbon nanotubes. Water Res. **39**, 1183–1189 (2005)

Mahdizadeh, S.J., Tayyari, S.F.: Influence of temperature, pressure, nanotube's diameter and intertube distance on methane adsorption in homogeneous armchair open-ended SWCNT triangular arrays. Theor. Chem. Acc. **128**, 231–240 (2011)

Mochida, I., Korai, Y., Shirahama, M.: Removal of SO_2 and NO_2 over activated carbon fibers. Carbon **38**, 227–239 (2000)

Peng, X., Li, Y., Luan, Z., Di, Z., Wang, H., Tian, B., Jia, Z.: Adsorption of 1, 2-dichlorobenzene from water to carbon nanotubes. Chem. Phys. Lett. **376**, 154–158 (2003)

Raymundo-Piñero, E., Cazorla-Amorós, D., Linares-Solano, A., Grulke, E., Andrews, R.: Temperature-programmed desorption study on the mecha- removal of SOx using polyacrylonitrile-based activated carbon fibres. Carbon **39**, 231–242 (2001)

Rodriguez-Reinoso, F.: The role of carbon materials in heterogeneous catalysis. Carbon **36**, 159–175 (1998)

Rubio, B., Izquierdo, M.T.: Influence of low-rank coal char properties on their SO_{-2} removal capacity from flue gases: 1 Non-activated char. Carbon **35**, 1005–1011 (1997)

Rubio, B., Izquierdo, M.T.: Low cost adsorbents for low temperature cleaning of flue gases. Fuel **77**, 631–637 (1998)

Sakizci, M., Alver, B.E., Yörükogullari, E.: Influence of the exchangeable cations on SO_{2-} adsorption capacities of clinoptilolite-rich natural zeolite. Adsorption **17**, 739–745 (2011)

Xin, Q., Luo, M.F.: Modern catalytic methods. Science Press, Beijing (2010)

Xu, H.: The prospect of clean coal technology. Clean coal technol. **13**, 89–92 (2007). In Chinese

Zawadzki, J.: Infrared studies of SO_2 on carbon-I, interaction of SO_2 with carbon films. Carbon **25**, 431–436 (1987)

Zhang, S.J., Shao, T., Bekaroglu, S.S.K., Karanfil, T.: The impacts of aggregation and surface chemistry of carbon nanotubes on the adsorption of synthetic organic compounds. Environ. Sci. Technol. **143**, 5719–5725 (2009)

Zhang, S.Y., Xiang, Y.H.: Study on the mechanism of flue gas desulfurization by carbonaceous materials. Coal Convers. **25**, 29–34 (2002). In Chinese

Zhang, S.Y., Zhu, T.Y., Wang, Y., et al.: Investigation on the desulfurization behavior of activated char. Power Syst. Eng. **20**, 47–51 (2004)